Journal of Solid State Chemistry **144,** 195–204 (1999)
Article ID jssc.1999.8148, available online at http://www.idealibrary.com on IDEAL®

Polymorphism in $Bi_5Pb_3O_{10.5}$

Akiteru Watanabe,[1] Yoshizo Kitami, and Satoshi Takenouchi

National Institute for Research in Inorganic Materials, 1-1 Namiki, Tsukuba, Ibaraki, 305-0044 Japan
E-mail: watanakt@nirim.go.jp

Jean-Claude Boivin

Laboratoire de Cristallochimie et Physicochimie du Solide, URA CNRS 452, ENSCL et USTL, BP108, 59652 Villeneuve d'Ascq, France

and

Nigel Sammes

Centre for Technology, The University of Waikato, Private Bag 3105, Hamilton, New Zealand

Received September 9, 1998; in revised form December 7, 1998; accepted December 10, 1998

This paper describes the phase and structural relations between three polymorphs of $Bi_5Pb_3O_{10.5}$. The low-temperature stable phase named β_L crystallizes in the triclinic system with $a = 14.903(1)$ Å, $b = 14.184(1)$ Å, $c = 7.2115(7)$ Å, $\alpha = 97.216(8)^\circ$, $\beta = 118.434(6)^\circ$, $\gamma = 80.647(8)^\circ$, and $Z = 4$. The unquenchable high-temperature stable phase labeled β forms a solid solution and has an anti-α-AgI-type structure with the space group $Im3m$; β-$Bi_5Pb_3O_{10.5}$ has $a = 4.40$ Å at 600°C and $Z = 2$ ($Bi_{5/8}Pb_{3/8}O_{10.5/8}$). The metastable phase termed β_2 also forms a solid solution and crystallizes in the tetragonal system with the possible space group $P4_2/n$; β_2-$Bi_5Pb_3O_{10.5}$ has $a = 12.132(1)$ Å, $c = 20.059(2)$ Å, and $Z = 9$. The β_L phase transforms to the β phase at about 585°C; on subsequent cooling, at about 560°C, the β phase changes to the β_2 phase which is kept to room temperature. The β_2 phase reverts to the β_L phase by annealing at low temperatures, e.g., at 500°C. The structure of β_L-$Bi_5Pb_3O_{10.5}$ is based on a pseudo-bcc β-type subcell, and the transformation matrix is $(-2, 2, 2)/(1, -1, 3)/(\frac{3}{2}, \frac{1}{2}, -\frac{1}{2})$. The structure of the β_2 phase is connected to that of red tetragonal PbO-type structure according to $(3, 0, 0)/(0, 3, 0)/(0, 0, 4)$. From the viewpoint of the lone pair of electrons on Bi^{3+} and Pb^{2+}, the metastability of the β_2 phase is discussed. © 1999 Academic Press

Key Words: **$Bi_5Pb_3O_{10.5}$; polymorphs; triclinic; anti-α-AgI-type structure; red PbO-type structure; lone pair of electrons.**

INTRODUCTION

Several investigators (1–7) examined the phase relations in the system Bi_2O_3-PbO to study either the polymorphism of Bi_2O_3 or new useful compounds; among other things, Boivin and Tridot (6) first determined a phase diagram over the whole composition range with subsolidus regions. In succession, Biefeld and White (7) checked this phase diagram from the practical viewpoint of sintering aids of ZnO-based varistors. Although two results were somewhat contradictory, the phase relations of a compound, $Bi_8Pb_5O_{17}$ (55.55 mol% PbO), almost conform with each other's diagrams. That is, both researchers described two stable polymorphs: the unquenchable high-temperature phase, labeled β (6), and the low-temperature phase, which is not characterized at all. (Hereafter we designate this low-temperature phase the β_L phase.) There is, however, a slight difference in the β_L-to-β transformation temperature between the two phase diagrams, i.e., about 585°C (6) and 605°C (7). Unlike the β_L phase, the β phase forms a wide solid-solution series $Bi_{2-2x}Pb_xO_{3-2x}$ ($0.49 \le x \le 0.70$ at 630°C (6)) having a body-centered cubic (bcc) symmetry with $a = 4.418$ Å at 60 mol% PbO and 625°C (7). At the same time, a tetragonal phase termed β_2 (6) was identified as a metastable state (7). The β_2 phase prepared by quenching the β phase also forms a series of solid solution in accordance with the β solid solution; tetragonal lattice parameters for β_2-$Bi_8Pb_5O_{17}$ were $a = 4.04$ Å and $c = 5.02$ Å (5). After that, since Honnart *et al.* (8) reported the remarkably high oxide-ion conductivity of the β phase ($\sigma > 1\ S\,cm^{-1}$ at 600°C), the polymorphism and thermal behavior of $Bi_8Pb_5O_{17}$ have been intensively re-examined (9–12) for the purpose of the stabilization of the β phase in the same way as the stabilized zirconia. As a result, according to Fee *et al.* (12), the β_2 phase seemed to be stable at low temperatures, and the β_L phase was identified as an intermediate phase. Nevertheless, the β phase is undoubtedly the high-temperature stable modification

[1]To whom correspondence should be addressed.

0022-4596/99 $30.00

with the bcc structure, because all the reported results (6–8, 10–12) were the same with respect to this phase. Thus, the inconsistencies exist in the relative thermal stability between two polymorphs (β_L and β_2), and very little is known about the structures of them.

In our re-examination of a phase equilibrium of $Bi_8Pb_5O_{17}$, we have found the correct composition not $Bi_8Pb_5O_{17}$ but $Bi_5Pb_3O_{10.5}$ (54.54 mol% PbO) which has three polymorphs of the triclinic low-temperature stable form (β_L), the bcc high-temperature stable modification (β), and the tetragonal metastable form (β_2).

EXPERIMENTAL PROCEDURES

The starting materials were 99.9% pure Bi_2O_3 (Iwaki Chemicals Ltd.) and PbO (Kojundo Chemical Laboratory Co., Ltd.). The desired proportions of $Bi_{2-2x}Pb_xO_{3-2x}$ ($x = 0.40$–0.58) were accurately weighed and thoroughly hand mixed in an agate mortar. The mixture was transferred into a covered gold crucible and heated in air to undergo a solid-state reaction. Heating conditions were between 500 and 550°C for 60 h or more to prepare the β_L phase and at 600°C for 10 h or more to the tetragonal β_2 phase on the basis of the results by Honnart *et al.* (8) who described the β_L-to-β transformation temperature at 590°C. At the end of the reaction, the product was quenched by an air stream to room temperature. In particular, for the β_L phase, the same heat treatment was repeated several times after intermediate grindings to complete the reaction. All samples were examined after every quenching process by X-ray powder diffraction (XRPD) method using Cu$K\alpha$ radiation and a diffracted-beam monochromator.

To check preliminary lattice parameters and the crystal system of the β_L form, Visser's indexing program (13) was applied to the observed XRPD data measured with continuous scanning method at a scanning rate of 0.4° min^{-1}. The 2θ values were corrected using the external standard of a Si powder. Using these results, the precise lattice parameters were calculated by the least-squares method (14).

The *in situ* measurement of structural changes between polymorphs with temperature was carried out by high-temperature XRPD using a combination of a Siemens D5000 diffractometer (CuKα radiation) and a Siemens HTK10 high-temperature device with a platinum sample holder, a heating–cooling rate of 300°C hr^{-1}, and an air gas flow.

A JEOL JEM-2000EX, electron microscope was employed to observe electron diffraction patterns of the β_2 modification. The well-sintered β_2 phase was lightly crushed in an agate mortar to be easily cleaved into layered fragments a few microns in size, and then the fragments were set on a carbon mesh supporting film.

The thermal behavior was checked by differential thermal analysis (DTA). About 50 mg of powder sample put in a platinum sample holder underwent heating–cooling cycles at a rate of 10°C min^{-1} in air to the maximum temperature of 620°C. The reference material was α-Al_2O_3 and the temperature accuracy was ± 3°C. Transition temperatures were determined from onsets of peaks on DTA curves during the heating cycle.

In order to confirm the composition of the prepared phases, chemical analyses were conducted using chelatometric titration with EDTA and a xylenol orange indicator.

The densities of the powder samples were measured using a gas pycnometer (Micromeritics Accupyc 1330). The sample weight was about 20 g.

RESULTS AND DISCUSSION

Phase Relations

Figure 1 shows a magnified portion of an XRPD pattern of $Bi_8Pb_5O_{17}$ equilibrated at 500°C. Although the pattern is almost the same as reported before (7, 8, 10, 12), the weak reflections indicated by arrows turned out to be due to Pb_3O_4 (15). This result suggests that a true single phase has to possess the Bi-richer composition than $Bi_8Pb_5O_{17}$. Thus, by changing x in $Bi_{2-2x}Pb_xO_{3-2x}$, we could obtain the pure compound β_L-$Bi_5Pb_3O_{10.5}$ ($x = 0.5454$) using the same heat treatment mehod as for $Bi_8Pb_5O_{17}$. In the Bi-rich region ($x < 0.5454$), we observed a mixture of β_L-$Bi_5Pb_3O_{10.5}$ and $Bi_{12}PbO_{19}$ (3, 4). Figure 2 represents an XRPD pattern of β_L-$Bi_5Pb_3O_{10.5}$. Furthermore, Fig. 3 exhibits DTA traces of β_L-$Bi_5Pb_3O_{10.5}$ and $Bi_8Pb_5O_{17}$; as can be seen, a small thermal effect due to Pb_3O_4 is observed in $Bi_8Pb_5O_{17}$ in contrast to the pure compound β_L-$Bi_5Pb_3O_{10.5}$. Seeing that a several-times longer heat treatment for preparation may lead to the compositional change by ignition loss, the composition of β_L-$Bi_5Pb_3O_{10.5}$ was checked by chemical analysis. The results were 45.41 $\pm$ 0.01 mol% Bi_2O_3 and 54.59 $\pm$ 0.01 mol% PbO. Since the

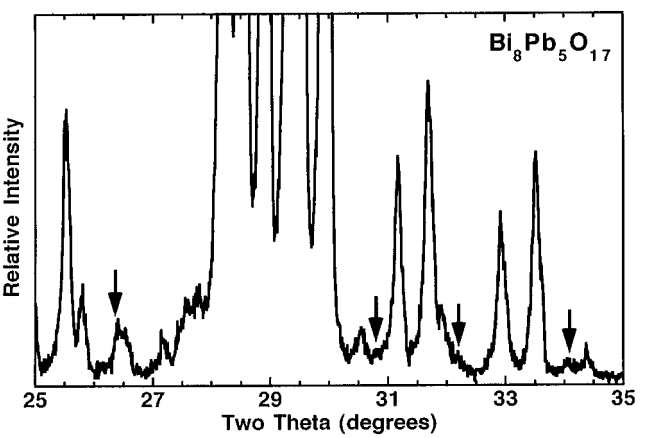

FIG. 1. Room-temperature XRPD pattern of $Bi_8Pb_5O_{17}$ equilibrated at 500°C (λ = Cu$K\alpha$). Reflections indicated by arrows are due to Pb_3O_4.

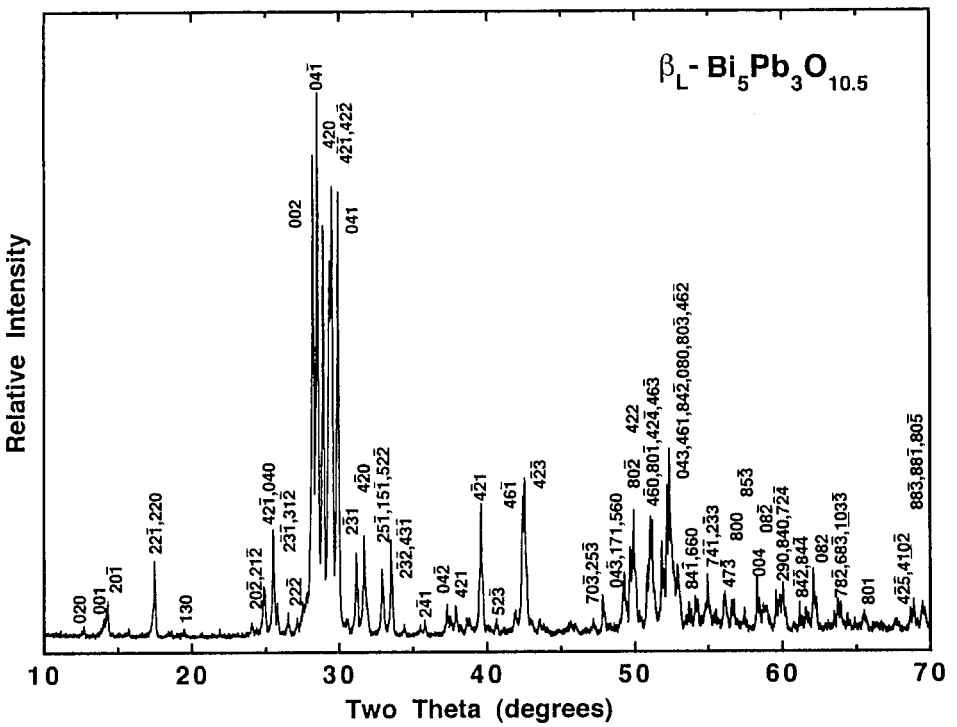

FIG. 2. Room-temperature XRPD pattern of β_L-$Bi_5Pb_3O_{10.5}$ equilibrated at 500°C ($\lambda = CuK\alpha$).

compositional change during the heat treatment is negligibly small, the actual composition is virtually equal to the nominal one. Thus, we identified the new composition β_L-$Bi_5Pb_3O_{10.5}$ as the intermediate line compound in the present system.

The heat treatment of β_L-$Bi_5Pb_3O_{10.5}$ at 600°C brought the β_2 phase which yields an XRPD pattern presented in Fig. 4. Nevertheless, we found that the β_2 phase easily transforms into the β_L phase after annealing at 500°C for 38 h. That is, the β_L phase can be generated by different ways through the solid-state reaction ($2.5Bi_2O_3 + 3PbO$) and through the β_2-to-β_L transformation. These results prove that the β_L phase is stable below the β_L-to-β transformation temperature as depicted in the phase diagrams (6,7). Consequently, the following experimental results of the β_L phase described by Fee *et al.* (12) are naturally observed in air: neither the annealing for 20 days at temperatures between 470 and 590°C nor the storage for 90 days at room temperature showed any structural change.

As for the β_2 phase, since this phase was possible to be prepared only on the conditions of the cooling process after the heat treatment above the β_L-to-β transformation temperature, we can conclude the β_2 phase to be metastable state pointed out by Biefeld and White (7) and Honnart *et al.* (8). In addition, Fee *et al.* (12) detected the β_2-to-β_L transition on the DTA trace which showed a broad exothermic peak around 480°C in the first heating direction. Generally, a phase transition between stable phases accompanies an endothermic effect in the heating process, so that the exothermic effect supports that the β_2 phase is metastable.

Figure 5 exhibits the results of high-temperature XRPD for β_L-$Bi_5Pb_3O_{10.5}$ as the starting compound. Although the resolution of reflections is lower than that of Fig. 2, we can clearly observe the structural change with temperature. The β_L phase transforms directly into the β phase in the first heating process. At 600°C, we can recognize the bcc symmetry ($a = 4.40$ Å) for the β phase as previously reported (7, 8, 10, 12) despite of a perceptible quantity of the β_L phase probably due to the temperature gradient on the sample holder. Once the β phase appears, a subsequent cooling process leads to the β_2 phase rather than the β_L phase under the present cooling rate (300°C h^{-1} = 5°C min^{-1}). At the end of the measurement, thus, we obtain the β_2 phase at room temperature. The same results were observed in the DTA measurement shown in Fig. 3b, where the β_L-to-β transformation at 587°C and the β-to-β_2 transformation at 563°C occur respectively in the heating and cooling cycle at a rate of 10°C min^{-1}. After the DTA measurement, the sample was characterized as the pure β_2 phase from a room-temperature XRPD result. Although the above results suggest that the β_L-to-β transformation is irreversible, this irreversibility is an ostensible phenomenon, because, as mentioned above, the β_2 phase transforms easily into the β_L phase by annealing at 500°C. Namely, since a rate of the β_2-to-β_L transformation is relatively sluggish, the β_2 phase is metastably quenched with ease even under the

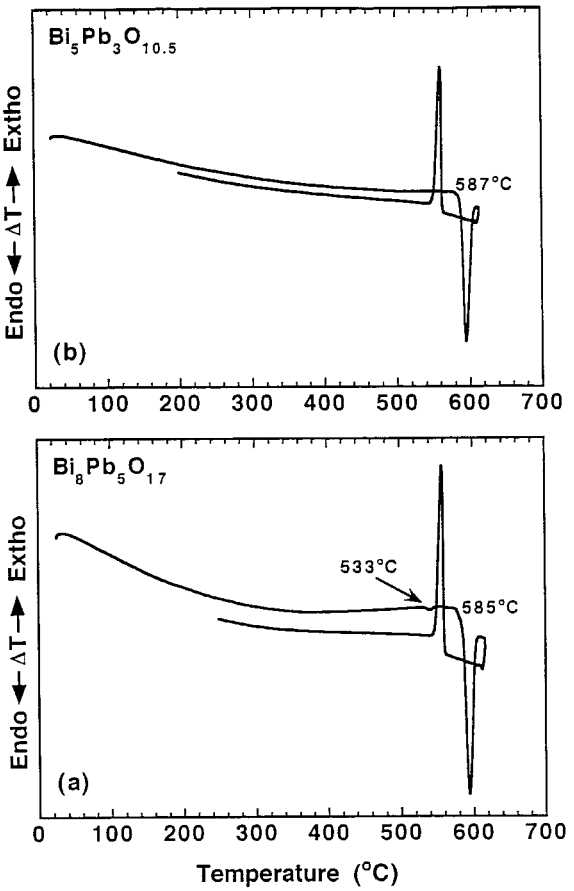

FIG. 3. DTA curves in the heating and cooling cycle for (a) $Bi_8Pb_5O_{17}$ and (b) $Bi_5Pb_3O_{10.5}$.

above cooling rate. However, upon heating the β_2 phase at a very slow rate, we can observe *in situ* the β_2-to-β_L transformation. In fact, Honnart *et al.* (8) reported a result of high-temperature XRPD taken by a Guinier-Lénne camera which is usually operated at a heating rate of 20°C h^{-1} or slower; their result clearly showed that β_2-$Bi_8Pb_5O_{17}$ transforms into the β_L phase (strictly speaking, β_L-$Bi_5Pb_3O_{10.5}$ and a very small amount of Pb_3O_4) at 450°C and subsequently the β_L-to-β transition occurs at 590°C. Likewise, inasmuch as Sammes *et al.* (10) observed the same transformation sequence in their high-temperature XRPD measurement, they erroneously identified the β_2 phase as the low-temperature stable modification and the β_L phase as the intermediate.

On the other hand, against expectation, we can recognize additional weak reflections at about $2\theta = 27.7°$, 32.3°, and 54.9° on the XRPD curves at 610°C in the first heating and at 600 and 610°C in the second heating in Fig. 5. These three reflections are attributed to the compound $Bi_{12}PbO_{19}$ (3, 4). This implies that the pure β phase exists at higher temperatures than 610°C. In other words, β_L-$Bi_5Pb_3O_{10.5}$ might undergo a peritectoid reaction, thereby resulting in two phases, i.e., $Bi_{12}PbO_{19}$ and the Pb-rich β phase in the heating direction. However, since this fact cannot be explained using the reported phase diagrams (6, 7), further investigaion on the phase equilibria will be the subject of future studies.

Structural Relations

The β solid solution. In the light of high oxide-ion conduction of the β phase, Honnart *et al.* (8) reported an anti-α-AgI-type structure for it. Graia *et al.* (16) determined the bcc structure of this type using the single crystal X-ray diffraction method applied to $Bi_{0.79}Cd_{0.21}O_{1.395}$ ($a = 4.281$ Å) which is one composition in a solid solution series $Bi_{1-x}Cd_xO_{1.5-x/2}$ ($0.11 < x < 0.25$); as a result, the space group was *Im*3*m* and $Z = 2$ with Bi and Cd atoms statistically distributed in (2*a*) with 0, 0, 0 and O atoms in (12*d*) with $\frac{1}{4}$, 0, $\frac{1}{2}$. The structure is depicted in Fig. 8c. Although the cations fully occupy their sites, the oxide-ions occupy only 23.25% ($= 1.395 \times 2/12$) of their sites which are shown as open squares in Fig. 8c. This numerous vacancies of the oxygen sublattice may give rise to the high oxide-ion conduction. Thus, the β solid solution $Bi_{2-2x}Pb_xO_{3-2x} = Bi_{(2-2x)/(2-x)}Pb_{x/(2-x)}O_{(3-2x)/(2-x)}$ is isomorphous with $Bi_{1-x}Cd_xO_{1.5-x/2}$.

The β_L compound. The indexing result of the computer program indicated that β_L-$Bi_5Pb_3O_{10.5}$ crystallizes in the triclinic system, and the precise lattice parameters were calculated: $a = 14.903(1)$ Å, $b = 14.184(1)$ Å, $c = 7.2115(7)$ Å, $\alpha = 97.216(8)°$, $\beta = 118.434(6)°$, $\gamma = 80.647(8)°$, and $V = 1320.6(1)$Å^3. The Miller indices based on these lattice constants are assigned to the reflections as shown in Fig. 2 and as listed in Table 1, which gives the observed and calculated d values and relative intensities with $I_{obs} \geq 2$. Since the measured density was 9.219(3) g cm^{-3}, it is obvious from this value and the cell volume that the triclinic cell contains four formula weights, $Z = 4(Bi_5Pb_3O_{10.5})$.

The XRPD pattern shown in Fig. 2 suggests that the triclinic β_L lattice is related to the above-mentioned bcc β lattice. That is, the triclinic structure forms a supercell based on a pseudo-bcc subcell. The fundamental reflections on the subcell are labeled $h'k'l'$ in Table 1. The comparison of the triclinic indices hkl with the pseudo-bcc ones $h'k'l'$ brought about the topotactic relationship between the two lattices. The result yielded the transformation matrix for the direct-lattice unit-cell vectors from the pseudo-bcc lattice (**a**′, $a' \approx 4.3$ Å) to the triclinic one (**a**, **b**, **c**): $(-2, 2, 2)/(1, -1, 3)/(\frac{3}{2}, \frac{1}{2}, -\frac{1}{2})$. Figure 6 exhibits these topotactic relations: $a \approx 2\sqrt{3}a'$, $b \approx \sqrt{11}a'$, and $c \approx (\sqrt{11}/2)a'$. The value of the determinant of the transformation, 16, implies that the volume of the triclinic cell is 16 times the size of the pseudo-bcc subcell. Since the bcc cell contains two lattice points at which the metal atoms, Bi and Pb, are randomly

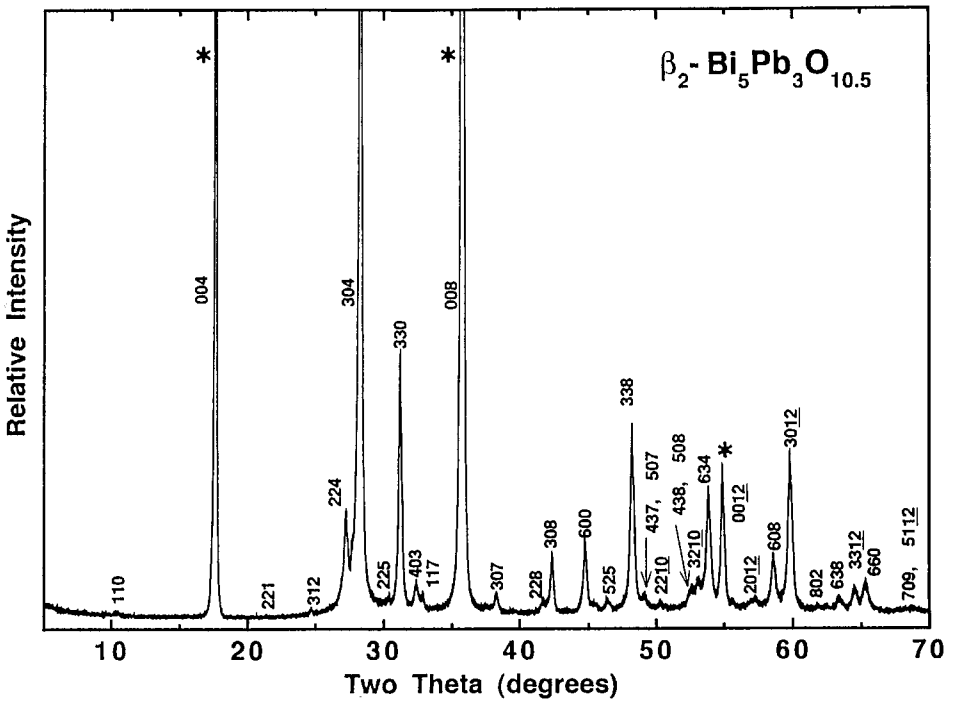

FIG. 4. Room-temperature XRPD pattern of β_2-$Bi_5Pb_3O_{10.5}$ ($\lambda = CuK\alpha$).

located, there are $2 \times 16 = 32$ lattice points in the triclinic cell. This result is in good agreement with the number of cations included in the triclinic cell, i.e., $Z = 4(Bi_5Pb_3O_{10.5})$. Thus, the formation of the triclinic phase might be due to the atomic ordering of Bi and Pb atoms. By contrast, the reported composition $Bi_8Pb_5O_{17}$ cannot satisfy this supercell–subcell lattice–points relationship.

Biefeld and White (7) described only the d values and relative intensities of 18 strong XRPD lines using Cu$K\alpha$ in the 2θ range between 25° and 84° for $Bi_8Pb_5O_{17}$ of which an XRPD pattern is the same as Fig. 1. As compared with Table 1, their results are too rough to characterize the triclinic symmetry. On the other hand, Bordovskii and Zarkoi (9) reported a monoclinic lattice with $a = 6.34$ Å,

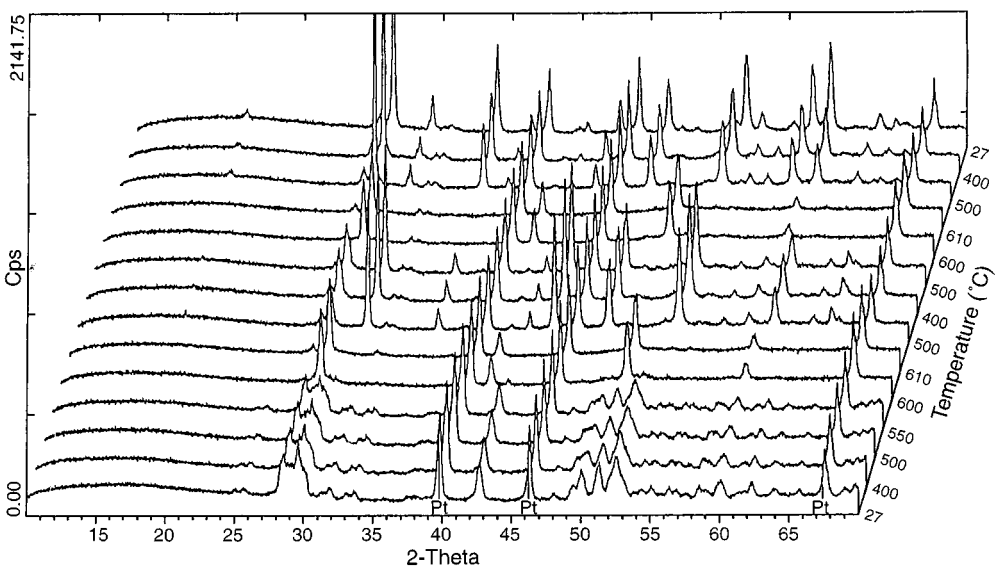

FIG. 5. Series of high-temperature XRPD patterns of $Bi_5Pb_3O_{10.5}$ ($\lambda = CuK\alpha$). Reflections designated by Pt's are due to the platinum sample holder.

TABLE 1
X-Ray Powder Diffraction Data for β_L-$Bi_5Pb_3O_{10.5}$

h	k	l	d_{calc} (Å)	d_{obs} (Å)	I_{obs}[a]	h'	k'	l'[b]
0	2	0	6.986	6.979	2			
0	0	1	6.331	6.323	4			
2	0	−1	6.206	6.203	6			
2	2	−1	5.079	5.073	15			
2	2	0	5.068					
1	3	0	4.559	4.562	2			
4	1	−1	3.703	3.702	2			
2	0	−2	3.576	3.575	9			
2	1	−2	3.575					
4	2	−1	3.495	3.492	20			
0	4	0	3.493					
2	−3	−1	3.458	3.456	6			
3	1	−2	3.453					
2	−1	−2	3.363	3.362	4			
2	2	−2	3.362					
3	2	−2	3.282	3.284	2			
4	1	0	3.254	3.254	4			
2	4	0	3.241	3.240	6			
3	−1	−2	3.216	3.210	8			
0	0	2	3.165	3.165	87	1	1	0
0	4	−1	3.133	3.131	100	0	1	−1
4	2	0	3.092	3.090	75	0	1	1
4	−2	−1	3.048	3.047	69	1	−1	0
4	2	−2	3.029	3.030	84	1	0	−1
0	4	1	2.989	2.989	83	1	0	1
4	−1	−2	2.927	2.929	3			
2	−3	1	2.871	2.870	15			
2	−4	−1	2.848	2.848	2			
4	−2	0	2.824	2.823	19			
4	3	−2	2.807	2.808	7			
3	2	1	2.803					
2	5	−1	2.724	2.723	13			
1	5	−1	2.723					
5	2	−2	2.702	2.716	9			
2	−3	−2	2.676	2.676	18			
4	−3	−1	2.676					
3	−4	−1	2.611	2.610	2			
0	5	−1	2.610					
4	−3	0	2.5310	2.5307	2			
2	−4	1	2.5123	2.5104	2			
0	4	−2	2.4135	2.4129	4			
2	1	2	2.3998	2.3995	3			
4	−1	1	2.3996					
4	2	1	2.3752	2.3746	5			
5	4	−2	2.3545	2.3544	2			
6	−1	−1	2.3322	2.3319	3			
4	2	−3	2.3190	2.3203	3			
4	−2	1	2.2766	2.2766	25	0	2	0
4	−4	0	2.2523	2.2512	2			
5	2	−3	2.2216	2.2223	3			
5	0	−3	2.2216					
4	3	−3	2.2216					
2	3	−3	2.1962	2.1970	2			
2	−3	2	2.1571	2.1580	4			
6	4	−1	2.1539	2.1533	4			
4	6	−1	2.1321	2.1319	26	0	0	2
4	−2	−3	2.1236	2.1247	29	2 0	0	
6	−1	0	2.1060	2.1054	3			
3	5	1	2.0994	2.0991	2			
4	4	1	2.0812	2.0810	2			
7	0	−2	2.0811					
2	6	−2	2.0764	2.0759	2			
0	1	3	2.0699	2.0694	2			
2	−6	−1	2.0699					
7	−1	−1	1.9976	1.9970	2			
3	−5	1	1.9875	1.9874	2			
4	−3	−3	1.9752	1.9762	2			
2	−6	1	1.9480	1.9467	2			
6	4	−3	1.9265	1.9264	3			
7	0	−3	1.9017	1.9012	8			
2	5	−3	1.9015					
4	7	−1	1.8894	1.8887	2			
4	0	2	1.8743	1.8738	2			
0	7	1	1.8742					
8	1	−2	1.8598	1.8603	3			
0	4	−3	1.8526	1.8523	10	1	2	−1
1	7	1	1.8480	1.8475	12			
5	6	0	1.8470					
8	0	−2	1.8353	1.8344	17			
4	2	2	1.8263	1.8270	23	1	2	1
8	3	−2	1.8126	1.8131	5			
4	−6	0	1.7963	1.7955	12	1	−2	1
8	0	−1	1.7890	1.7889	21	1	−2	−1
4	2	−4	1.7878			2	1	−1
4	6	−3	1.7844	1.7842	22	1	1	−2
0	4	3	1.7636	1.7637	17	2	1	1
4	6	1	1.7529	1.7526	13	1	1	2
8	4	−2	1.7479	1.7474	34	1	−1	−2
0	8	0	1.7467			1	−1	2
8	0	−3	1.7376	1.7375	13	2	−1	−1
4	−6	−2	1.7293	1.7294	12	2	−1	1
2	−5	−3	1.7146	1.7143	4			
7	5	−3	1.7140					
6	−5	−1	1.7078	1.7077	5			

[a] Weak reflections (< 2) are omitted to reduce the table.
[b] Miller indices based on the pseudo-bcc subcell.

$b = 8.09$ Å, $c = 9.45$ Å, and $\beta = 97.1°$ for $Bi_8Pb_5O_{17}$ similar to the above phase (7) on the basis of 13 reflections on Cu$K\alpha$ within the 2θ range from 5 to 70°. Lately, Fee *et al.* (12) checked the same phase $Bi_8Pb_5O_{17}$ using a transmission electron microscope (TEM); as a result, they wrote that this material consists of three distinct phases. As shown in Fig. 1, however, $Bi_8Pb_5O_{17}$ is composed of two phases, i.e., a major part of β_L-$Bi_5Pb_3O_{10.5}$ and a very small amount of Pb_3O_4. Accordingly the lowest symmetry of β_L-$Bi_5Pb_3O_{10.5}$ may mislead the TEM observation.

The metastable β_2 solid solution. To date, the β_2 phase has been described as tetragonal lattices: $a = 4.026$ Å and $c = 5.077$ Å at 60 mol% PbO (5); $a = 4.041$ Å and

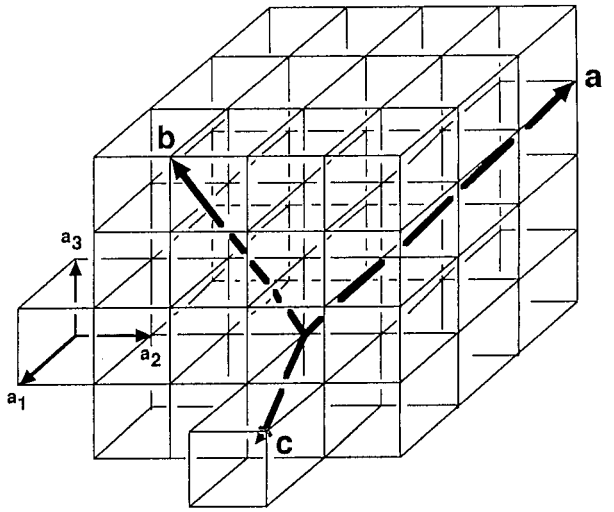

FIG. 6. Schematic representation of the unit-cell axis relations between the triclinic cell (**a**, **b**, **c**) of β_L-$Bi_5Pb_3O_{10.5}$ and the pseudo-bcc subcell ($\mathbf{a}_1$, $\mathbf{a}_2$, $\mathbf{a}_3$) related to the β phase. Cations might occur at about pseudo-cube corners and body centers.

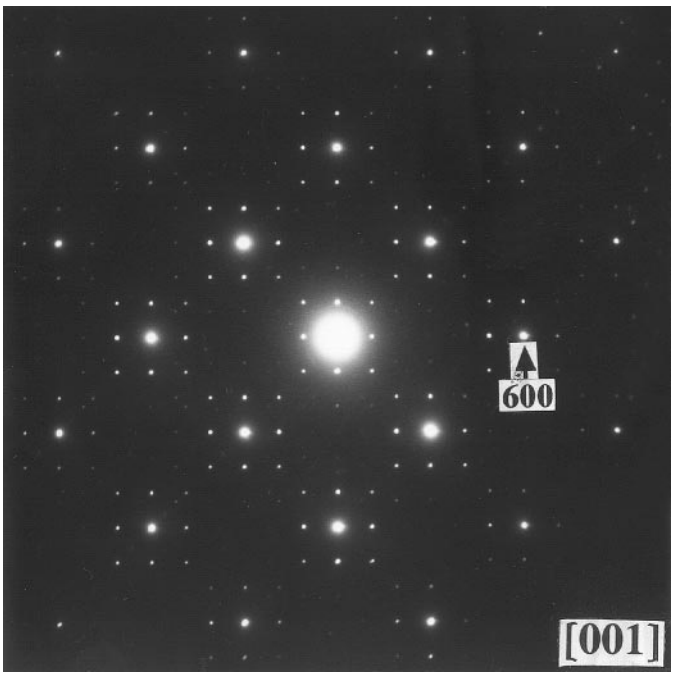

FIG. 7. Electron diffraction pattern of β_2-$Bi_5Pb_3O_{10.5}$ in the [001] orientation.

$c = 5.023$ Å at 55.55 mol% PbO (8); $a = 5.76$ Å and $c = 9.40$ Å at 55.55 mol% PbO (9), $a = 4.0434$ Å and $c = 5.0178$ Å at 55.55 mol% PbO (17); and $a = 24.246$ Å and $c = 5.015$ Å at 55.59 mol% PbO (18). Nevertheless, none of these lattices explain the XRPD pattern presented in Fig. 4 because almost all the weak reflections were ignored.

Figure 7 exhibits an electron diffraction photograph of β_2-$Bi_5Pb_3O_{10.5}$ in the [001] orientation. A tetragonal symmetry is clearly indicated by the array of strong diffraction spots from which we can be read the same value (4.06 Å) as the a axis length mentioned above. At the same time, we can see the incommensurate reflections which suggest a certain distortion of a unit cell. Likewise, for a sample with composition of 37.45 mol% PbO, an electron diffraction result showed the same pattern including the incommensurate spots. So that the modulated structure is characteristic of the β_2 phase. However, we employed only the strong spots at present. As mentioned in the experimental section, since the β_2 phase has remarkably layered morphology, we could not observe the minute fragments in other orientations. For this reason, we could not obtain any information about the c-axis from electron diffraction. On the contrary, the layered morphology yielded reinforced 00l reflections on XRPD owing to the preferred orientation effect. Actually, we can easily observe the effect in Fig. 4; namely, the asterisked reflections mean the exaggerated 00l lines. If the index 001 is assigned to the lowest angle 00l reflection at $2\theta = 17.7^\circ$, the c axis length is calculated to be 5.01 Å, the same value as above.

On the other hand, Boivin *et al.* (5) pointed out that the XRPD pattern of the β_2 phase bears close resemblance to that of a red (tetragonal) form of PbO which crystallizes in the space group $P4/nmm$ with $a = 3.9729$ Å and $c = 5.0217$ Å (19, 20) and has a layer structure with the stereochemically active lone pairs of electrons ($6s^2$) on Pb^{2+} ions (21). Likewise, Bi_2O_3 is possible to have the same configuration as red PbO in the form of $(Bi_2O_2)^{2+}$ with the Bi^{3+} lone pair in many layered compounds of the Aurivillius family $(Bi_2O_2)^{2+}(A_{n-1}B_nO_{3n+1})^{2-}$ where A is a combination of ions for twelve-coordinated interstices, B is a combination of ions for octahedrally coordinated sites, and n is an integer between 1 and 5 (22). Moreover, as mentioned above, the β_2 phase has the layered morphology. Thus, in view of these known results, we examined a structure of the β_2 phase on the basis of red PbO structure which is presented in Fig. 8a. That is, since the strong X-ray reflections from the β_2 phase (Fig. 4) agree with those from red PbO, a possible unit cell of the β_2 phase may be a superstructure based on a red-PbO-type subcell. As a result, the tetragonal cell with $a = 12.132(1)$ Å and $c = 20.059(2)$ Å explained well the whole XRPD pattern for β_2-$Bi_5Pb_3O_{10.5}$ as indexed in Fig. 4; in addition, Table 2 lists the observed and calculated d values and intensities of XRPD lines along with the corresponding Miller indices $h'k'l'$ of the red-PbO-related subcell. The observable reflections are hkl, all orders; $hk0$, $h + k = 2n$; and 00l, $l = 2n$. These conditions lead to the possible space group $P4_2/n$. The transformation matrix from the red-PbO-type sublattice (**a**′ and **c**′, $a' \approx 4.04$ Å and $c' \approx 5.01$ Å) to the superlattice (**a** and **c**) can be expressed as

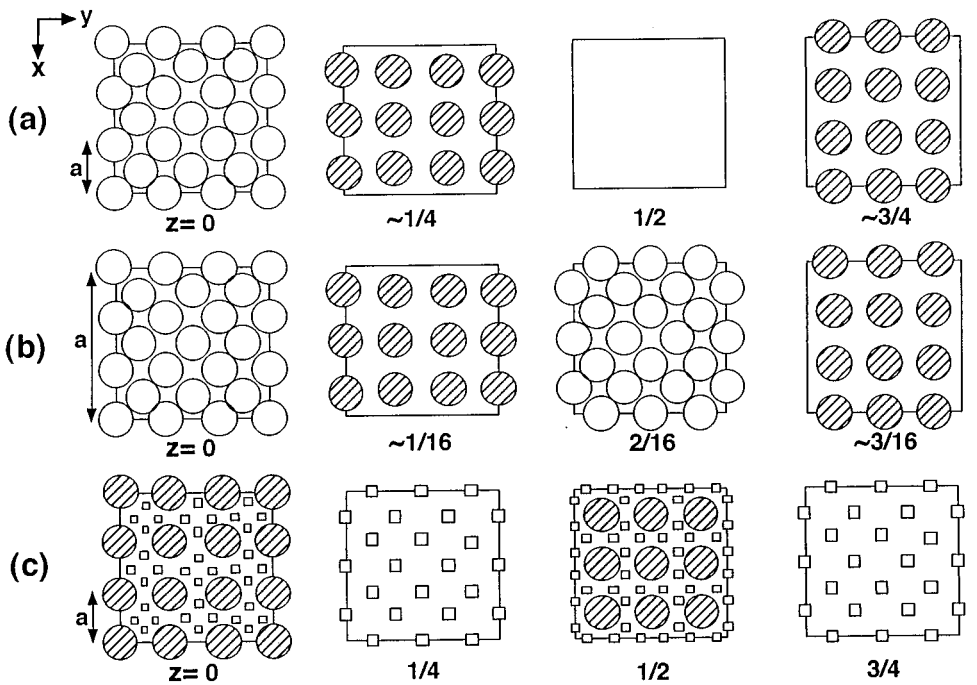

FIG. 8. Crystal structures presented in a series of cross sections. Open circles are oxygen atoms in common. (a) Nine unit cells of tetragonal red PbO structure with $P4/nmm$: hatched circles are Pb atoms. (b) Proposed structure of the β_2 solid solution based on $P4_2/n$: hatched circles are metal atoms (Bi and Pb) which occupy two sets of (4*e*) and eight sets of (8*g*) positions. (c) Nine unit cells of the β solid solution with anti-α-AgI-type structure: hatched circles are metal atoms (Bi and Pb) distributed randomly in (2*a*) positions of $Im3m$, and open squares are possible sites for oxygen atoms.

(3, 0, 0)/(0, 3, 0)/(0, 0, 4), i.e., $a \approx 3a'$ and $c \approx 4c'$. Seeing that the unit cell of red PbO contains two formula weights (Fig. 8a), we note that there exist 72 ($= 2 \times 3 \times 3 \times 4$) cations in the unit cell of the β_2 phase. Actually, in the case of β_2-$Bi_5Pb_3O_{10.5}$, the measured density 9.190(2) g cm^{-3} and the cell volume 2952.5(6) Å^3 result in $Z = 9$, i.e., 45 Bi atoms and 27 Pb atoms, and the sum total 72 cations. In general, the number of bismuth, lead, and oxygen atoms in the β_2 unit cell can be calculated from the chemical formula, $Bi_{2-2x}Pb_xO_{3-2x} = Bi_{(2-2x)/(2-x)}Pb_{x/(2-x)}O_{(3-2x)/(2-x)}$. They are $72[(2-2x)/(2-x)]$ Bi's, $72[x/(2-x)]$ Pb's, and $72[(3-2x)/(2-x)]$ O's.

According to the symmetry of $P4_2/n$ (No. 86) (23), as shown in Fig. 8b, all 72 cations were assigned to the following sites ($z = \sim n/16$ where $n = 1, 3, 5, \ldots, 15$) similar configuration to red PbO: two sets of the special positions 4*e* and eight sets of the general positions 8*g*. The ordering of cations (Bi or Pb) may bring about the superstructure. Each cross section at $z = \sim n/16$ contains nine cations, so that the total number of cations are $9 \times 8 = 72$. As for the oxide ions, just 72 oxygen atoms were placed at the same positions ($z = n/16$ where $n = 0, 4, 8, 12$) as red PbO, i.e., the special positions 2*a*, 2*b*, and 4*f*, and eight sets of the general positions 8*g*. Note that each cross section contains 18 oxygen atoms. An excess of oxide ions of which the number is $72[(1-x)/(2-x)]$ need to be distributed in the interstices ($z = n/16$ where $n = 2, 6, 10, 14$) corresponding to the space at $z = \frac{1}{2}$ in red PbO (Fig. 8a) where no oxide ion exists because the Pb^{2+} lone pair faced each other within this space (21). Two sets of the special positions 4*e* and nine sets of the general positions 8*g* were allocated to these excess oxide ions. Thus, Fig. 8b shows an inferable structure of the β_2 phase where a series of cross sections within $0 \le x \le 1$, $0 \le y \le 1$, and $0 \le z \le \frac{1}{4}$ are depicted. Nevertheless, a true structure of the β_2 phase is incommensurate as evidenced in Fig. 7, so that this problem will also be the future subject.

Assuming that the excess oxide ions occupy their sites statistically, the occupancy factor is $(1-x)/(2-x)$. For instance, in $Bi_5Pb_3O_{10.5}$ ($x = 0.5454$), the factor is calculated to be 0.3125. The presence of these excess oxide ions interleaved with the Pb^{2+} and Bi^{3+} lone-pair layers seems to make the β_2 phase metastable, because the stereochemically active lone-pair electrons interact repulsively on oxide ions (24). In addition, as compared with the anti-α-AgI-type β phase structure (Fig. 8c), the proposed structure of the β_2 phase is easily connected to that of the β phase. Namely, in the β phase, every other oxygen layer (e.g., $z = \frac{1}{4}$) is fully occupied, at the same time, the cation layers ($z = 0$ and $\frac{1}{2}$) situated on both sides slightly shift towards this fully packed oxygen layer, and the other oxygen atoms occupy the rest oxygen layer ($z = \frac{3}{4}$). By this relatively simple moving of atoms, the β phase changes to the β_2 phase. Therefore,

TABLE 2
X-Ray Powder Diffraction Data for β_2-$Bi_5Pb_3O_{10.5}$

h	k	l	d_{calc} (Å)	d_{obs} (Å)	I_{obs}	h'	k'	l'[a]
1	1	0	8.578	8.503	1			
0	0	4	5.014	5.009	55	0	0	1
2	2	1	4.194	4.159	1			
3	1	2	3.583	3.595	1			
2	2	4	3.259	2.265	5			
1	0	6	3.223	3.214	3			
3	0	4	3.147	3.147	47	1	0	1
2	2	5	2.929	2.934	1			
3	3	0	2.859	2.858	11	1	1	0
4	0	3	2.762	2.759	2			
1	1	7	2.717	2.718	1			
0	0	8	2.5073	2.5059	100	0	0	2
4	2	4	2.3860	2.3895	1			
3	0	7	2.3380	2.3463	1			
2	1	8	2.2760	2.2742	1			
2	2	8	2.1646	2.1642	1			
4	4	0	2.1446	2.1477	1			
3	0	8	2.1310	2.1303	3	1	0	2
6	0	0	2.0220	2.0219	3	2	0	0
0	0	10	2.0059	2.0029	1			
5	2	5	1.9643	1.9645	1			
1	1	10	1.9532	1.9523	1			
3	0	9	1.9519					
3	3	8	1.8852	1.8848	8	1	1	2
4	3	7	1.8517	1.8506	1			
5	0	7	1.8517					
2	2	10	1.8170	1.8125	1			
4	3	8	1.7436	1.7436	1			
5	0	8	1.7436					
3	2	10	1.7229	1.7231	2			
6	3	4	1.7012	1.7021	5	2	1	1
0	0	12	1.6715	1.6712	6	0	0	3
6	0	7	1.6521	1.6517	1			
7	2	3	1.6169	1.6157	1			
4	2	10	1.6128					
2	0	12	1.6115	1.6072				
6	0	8	1.5739	1.5741	3	2	0	2
3	0	12	1.5448	1.5446	7	1	0	3
8	0	2	1.4994	1.4997	1			
2	1	13	1.4841	1.4847	1			
6	3	8	1.4667	1.4673	1	2	1	2
3	3	12	1.4431	1.4432	1	1	1	3
6	6	0	1.4297	1.4287	1	2	2	0
7	0	9	1.3681	1.3681	1			
5	1	12	1.3677					
6	5	7	1.3656	1.3649	1			
4	4	12	1.3184	1.3183	1			
9	0	4	1.3017	1.3018	1	3	0	1
6	0	12	1.2883	1.2884	1	2	0	3
9	3	0	1.2788	1.2783	1	3	1	0
0	0	16	1.2536	1.2537	1	0	0	4
6	6	8	1.2420	1.2405	1	2	2	2
9	3	4	1.2391	1.2368	1	3	1	1
6	3	12	1.2275	1.2280	1	2	1	3
3	0	16	1.1974	1.1972	1	1	0	4
9	0	8	1.1872	1.1838	1	3	0	2
3	3	16	1.1481	1.1482	1	1	1	4
9	3	8	1.1392	1.1381	1	3	1	2
9	6	4	1.0945	1.0947	1	3	2	1
6	6	12	1.0865	1.0856	1	2	2	3
3	0	18	1.0743	1.0739	1			
6	0	16	1.0655	1.0652	1	2	0	4
3	2	18	1.0578	1.0571	1			
9	0	12	1.0493	1.0490	1	3	0	3
6	3	16	1.0303	1.0308	1	2	1	4
9	6	8	1.0238	1.0238	1	3	2	2
12	0	0	1.0110	1.0111	1	4	0	0
0	0	20	1.0029	1.0031	1	0	0	5

[a] Miller indices based on the red-PbO-type subcell.

from the close structural relation between the β and β_2 phases, it might be understood that the cubic β phase preferentially transforms into the tetragonal β_2 phase rather than directly into the triclinic β_L phase. On the contrary, the atom ordering into the triclinic β_L phase would seem to be somewhat time-consuming process, because the rate of the β_2-to-β_L transformation is actually sluggish.

ACKNOWLEDGMENT

One of authors (A. Watanabe) thanks Ms. Laurence Burylo with Laboratoire de Cristallochimie et Physcochimie du Solide for high-temperature XRPD measurement.

REFERENCES

1. L. Belladen, *Gass. Chem. Ital.* **52,** 160 (1922).
2. I. M. Belyaev and N. P. Smolyaninov, *Russ. J. Inorg. Chem.* **7,** 579 (1962).
3. B. Aurivillius and L. G. Sillén, *Nature* (*London*) **155,** 305 (1945).
4. E. M. Levin and R. S. Roth, *J. Res. Nat. Bur. Stand. Sect. A* **68,** 197 (1964).
5. J. C. Boivin, D. Thomas, and G. Tridot, *C. R. Acad. Sci., Paris, Ser. C* **268,** 1149 (1969).
6. J. C. Boivin and G. Tridot, *C. R. Acad. Sci., Paris, Ser. C* **278,** 865 (1974).
7. R. M. Biefeld and S. S. White, *J. Am. Ceram. Soc.* **64,** 182 (1981).
8. F. Honnart, J. C. Boivin, D. Thomas, and K. J. De Vries, *Solid State Ionics* **9/10,** 921 (1983).
9. G. A. Bordovskii and A. B. Zarkoi, *Phys. Stat. Sol. A* **87,** K7 (1985).
10. N. M. Sammes, R. J. Phillips, and M. G. Fee, *Solid State Ionics* **69,** 121 (1994).
11. N. M. Sammes, G. Tompsett, and A. M. Cartner, *Solid State Commun.* **96,** 545 (1995).
12. M. G. Fee, N. M. Sammes, G. Tompsett, T. Stoto, and A. M. Cartner, *Solid State Ionics* **95,** 183 (1997).
13. J. W. Visser, *J. Appl. Crystallogr.* **2,** 89 (1969).
14. D. E. Appleman and H. T. Evans, Jr., *NTIS* **PB-216,** 188 (1973).
15. Powder Diffraction File, No. 8-19, International Center for Diffraction Data, Swarthmore, PA.
16. T. Graia, P. Conflant, G. Nowogrocki, J. C. Boivin, and D. Thomas, *J. Solid State Chem.* **63,** 160 (1986).

17. Powder Diffraction File, No. 41-405, International Center for Diffraction Data, Swarhmore, PA.
18. Powder Diffraction File, No. 45-291, International Center for Diffraction Data, Swarthmore, PA.
19. J. Leciejewicz, *Acta Crystallogr*. **14,** 1304 (1961).
20. Powder Diffraction File, No.5-561, International Center for Diffraction Data, Swarthmore, PA.
21. A. F. Wells, "Structural Inorganic Chemistry," 4th ed., pp. 218 and 461. Clarendon, Oxford, 1975.
22. E. C. Subbarao, *J. Phys. Chem. Solids* **23,** 665 (1962).
23. N. F. M. Henry and K. Lonsdale, "International Tables for X-Ray Crystallography," Vol. I. Kynoch Press, Birmingham, UK, 1976.
24. A. Watanabe, *Mater. Res. Bull.* **19,** 877 (1984).